Fiber optic Fabry-Perot sensor for surface tension analysis

Violeta A. Márquez-Cruz* **and Juan A. Hernández-Cordero**

Instituto de Investigaciones en Materiales, Universidad Nacional Autónoma de México, Circuito Exterior s/n Ciudad Universitaria, Coyoacán D.F. 04510, Mexico

*violeta.marquez@gmail.com

Abstract: We demonstrate a new technique for analyzing surface tension of liquids. This is done upon examining the interference signals reflected from a remnant drop pending at the cleaved end of a single mode optical fiber. The resulting interference patterns are fitted to a multimirror Fabry-Perot model yielding information of the drop size. We show that the wetting process of the fiber plays an important role in drop formation; in particular, the drop size can be correlated to the surface tension of the liquid sample. The proposed configuration may render useful for liquids analysis using small sample volume.

OCIS codes: (060.2370) Fiber optics sensors; (120.2230) Fabry-Perot; (120.3180) Interferometry; (160.4760) Optical properties; (280.4788) Optical sensing and sensors.

References and links

1. P. G. de Gennes, F. Brochard-Wyart, and D. Quéré, *Capillarity and Wetting Phenomena. Drops, Bubbles, Pearls, Waves* (Springer Science + Business Media, Inc., 2004). Chap. 1, 2.
2. T. Young, "An essay on the cohesion of fluids," Phil. Trans. R. Soc. **95**(0), 65–87 (1805).
3. P. S. Laplace, *Théorie de l'action capillaire: Supplément au dixième livre du traité de mécanique céleste* (Duprat, 1808).
4. Y. Park, C. A. Best, K. Badizadegan, R. R. Dasari, M. S. Feld, T. Kuriabova, M. L. Henle, A. J. Levine, and G. Popescu, "Measurement of red blood cell mechanics during morphological changes," Proc. Natl. Acad. Sci. U.S.A. **107**(15), 6731–6736 (2010).
5. X. Xu, A. Jagota, S. Peng, D. Luo, M. Wu, and C. Y. Hui, "Gravity and surface tension effects on the shape change of soft materials," Langmuir **29**(27), 8665–8674 (2013).
6. A. Marmur, "Solid-surface characterization by wetting," Annu. Rev. Mater. Res. **39**(1), 473–489 (2009).
7. W. A. Wakeham, M. J. Assael, A. Marmur, J. de Coninck, T. D. Blake, S. A. Theron, and E. Zussman, "Material Properties: Measurement and Data", in *Handbook of Experimental Fluid Mechanics*, C. Tropea, A. L. Yarin, and J. F. Foss, eds. (Springer-Verlag Berlin Heidelberg, 2007).
8. A. F. Stalder, T. Melchior, M. Müller, D. Sage, T. Blu, and M. Unser, "Low-bond axisymmetric drop shape analysis for surface tension and contact angle measurements of sessile drops," Colloids Surf. A Physicochem. Eng. Asp. **364**(1-3), 72–81 (2010).
9. I. Flammer and J. Rička, "Dynamic light scattering with single-mode receivers: partial heterodyning regime," Appl. Opt. **36**(30), 7508–7517 (1997).
10. G. Popescu and A. Dogariu, "Dynamic light scattering in localized coherence volumes," Opt. Lett. **26**(8), 551–553 (2001).
11. A. Zhou, Z. Liu, and L. Yuan, "Fiber-optic dipping liquid analyzer: theoretical and experimental study of light transmission," Appl. Opt. **48**(36), 6928–6933 (2009).
12. A. Zhou, J. Yang, B. Liu, and L. Yuan, "A fiber-optic liquid sensor for simultaneously measuring refractive index, surface tension, contact angle and viscosity," Proc. SPIE **7503**, 75033B (2009).
13. Q. Song, G. X. Zhang, and Z. R. Qiu, "Review of drop analysis technology for liquid property study," Opto-Electron. Rev. **13**(1), 1–8 (2005).
14. N. D. McMillan, P. Davern, V. Lawlor, M. Baker, K. Thompson, J. Hanrahan, M. Davis, J. Harkin, M. Bree, P. Goossens, S. Smith, D. Barratt, R. Corden, D. G. E. McMillan, and D. Lane, "The instrumental engineering of a polymer fibre drop analyser for both quantitative and qualitative analysis with special reference to fingerprinting liquids," Colloids Surf. A Physicochem. Eng. Asp. **114**, 75–97 (1996).
15. C. Pigot and A. Hibara, "Surface tension measurement at the microscale by passive resonance of capillary waves," Anal. Chem. **84**(5), 2557–2561 (2012).
16. R. Wang, T. Kim, M. Mir, and G. Popescu, "Nanoscale fluctuations and surface tension measurements in droplets using phase-resolved low-coherence interferometry," Appl. Opt. **52**(1), A177–A181 (2013).

#201124 - $15.00 USD Received 11 Nov 2013; revised 16 Jan 2014; accepted 27 Jan 2014; published 3 Feb 2014

17. A. W. Adamson and A. P. Gast, *Physical Chemistry of Surfaces* (John Wiley and Sons, 6th edition, 1997). Chap. 2, 3, 10, 12.
18. K. Kim, S. Chang, and K. Oh, "Refractive microlens on fiber using UV-curable fluorinated acrylate polymer by surface-tension," IEEE Photon. Technol. Lett. **15**(8), 1100–1102 (2003).
19. J. Drelich, C. Fang, and C. L. White, "Measurement of interfacial tension in fluid-fluid systems," in *Encyclopedia of Surface and Colloid Science, Volume 3,* A. T. Hubbard, ed. (Marcel Dekker Inc., 2002), pp. 3158–3163.
20. H. van de Stadt and J. M. Muller, "Multimirror Fabry-Perot interferometers," J. Opt. Soc. Am. A **2**(8), 1363–1370 (1985).
21. V. A. Marquez-Cruz and J. Hernandez-Cordero, "Fiber optic multimirror Fabry-Perot sensor for liquids analysis," in *Latin America Optics and Photonics Conference*, OSA Technical Digest (online) (Optical Society of America, 2012), paper LS3B.2.
22. G. Datasheet and S. Fluids, Stable, Inert Media. Gelest, Inc, (1998).
23. Glycerol, product datasheet, Sigma Aldrich (2013). *http://www.sigmaaldrich.com/catalog/product/sial/g9012?lang=es&region=MX*.
24. J. A. Dean, *Lange's Handbook of Chemistry* (McGraw-Hill Inc., 15th edition, 1999), pp. 5.97.
25. V. F. Weisskopf, "Search for simplicity: mountains, water waves, and leaky ceilings," Am. J. Phys. **54**(2), 110 (1986).
26. M. Alonso, "Water drops and wet ceilings," Am. J. Phys. **54**(8), 679 (1986).

1. Introduction

The formal study of interfaces started with T. Young and P. S. Laplace in the early 19th century [1–3]. Since then, surface tension and wetting phenomena have been closely observed. These physical properties of liquids are of interest in many fields, such as the characterization of red blood cells [4], hydrogels drugs delivery or the study of rheology at micro or nanoscales, where surface effects dominate the volume properties [5]. Numerous measurement techniques have been developed to measure surface tension [1, 6]; some of them involve the study of drops, in different configurations, such as the pendant drop methods [7], or the measurement of contact angle of sessile drops, based on the Young-Laplace equation [8]. Optical techniques in particular have shown to be useful in the study of surface phenomena; for instance, characterization of colloidal suspensions [9, 10] and measurement of surface tension have been carried out using intensity based techniques, dynamic scattering analysis or optical coherence tomography [11–16]. In general, optical techniques are attractive owing to their non-contact capabilities and the small volume samples involved in the measurements.

The interest in surface tension measurements arises from the fact that changes at the molecular level will alter the physical properties of a liquid at the macroscopic level. Chemicals such as surfactants will induce changes in the surface tension and this may be used as a means for analyzing the concentration of surfactant in a liquid or in binary solutions [17]. Simple methods for monitoring surface tension variations are thus of interest for these kind of applications. In this paper, we propose a new and simple technique for measuring surface tension of a small drop using optical interferometry. By dipping the cleaved end of a single-mode optical fiber into a liquid, a tiny drop is formed whose dimensions are mainly determined by the surface tension of the liquid. The height of the drop is measured by means of the back-reflected signal from the drop to an optical interrogator. Analysis of the optical signal is carried out upon fitting the experimental data to a Fabry-Perot interferometer model, yielding information related to the drop height. The resulting drop heights for different liquids show to have a close relation mainly with the surface tension of the tested fluids.

2. Drop formation at the tip of an optical fiber

Drop formation at the tip of an optical fiber probe has been used for applications ranging from refractive index measurement of binary solutions to fiber device fabrication [11, 18]. In general, drops are readily formed upon immersing the tip of the optical fiber probe into the fluid of interest or by depositing the liquid on the cleaved surface of the optical fiber. While the measurement of refractive index does not require a strict analysis of the drop formation,

#201124 - $15.00 USD Received 11 Nov 2013; revised 16 Jan 2014; accepted 27 Jan 2014; published 3 Feb 2014

fabrication of polymer lenses in fiber tips involves important features of the polymer such as the viscosity and the initial volume [18]. Surface tension measurements, however, require a closer look to the drop formation on a finite solid surface. It is customarily assumed that relevant features in a wetting problem such as contact angle and drop geometry can be modeled following the Young-Laplace formulation [1, 6, 17]. However, optical fiber wetting processes and subsequent drop formation at the tip of the waveguide will not necessarily follow this classical approach, as shown in Fig. 1. This is particularly important if surface tension measurements are sought, because the dimensions of the drop formed with these arrangements are typically in the micron range.

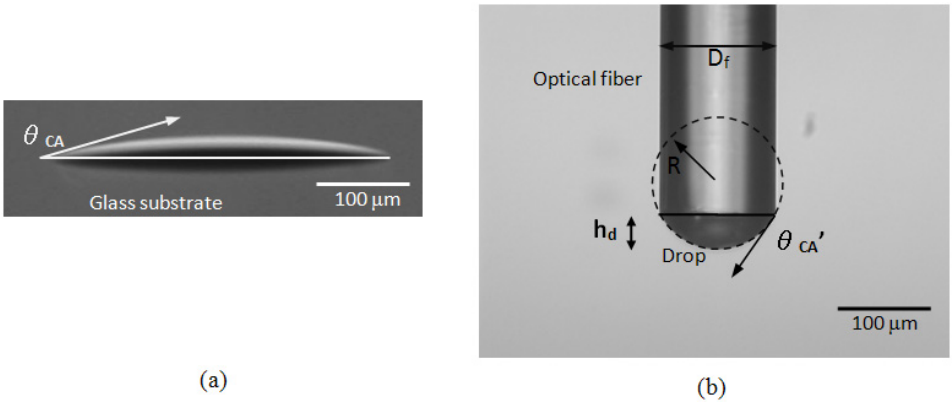

Fig. 1. (a) Contact angle of a sessile drop where Young-Laplace methods are frequently used; θ_{CA} is the contact angle. (b) Geometry of the remnant-pendant drop at the fiber end, where θ_{CA}' is the contact angle, h_d and R are respectively the height and the radius of curvature of the drop, and D_f is the diameter of the optical fiber.

Figure 1 illustrates two cases for drop formation on solid surfaces: while Fig. 1(a) shows a drop of a liquid formed on a flat glass surface, Fig. 1(b) depicts the case for a drop formed at the tip of an optical fiber. Notice that in spite of being the same liquid, and in principle, the same kind of solid surface, drop features such as size and contact angle are noticeably different. This is due to the finite size of the fiber end face, constraining the drop formation to a given volume, which as we will demonstrate, depends mostly on the surface tension of the liquid. It is worthwhile noticing that drop formation under these conditions is still an unsolved problem. The geometries that are traditionally analyzed (e. g., in the drop weight method or the sessile drop for contact angle measurement [1, 17, 19]) do not consider relevant effects for the proposed configuration. In particular, the work of adhesion on the cross section of the fiber, or the effect of a confined substrate on the drop dimensions, are still to be considered in complete analysis of this wetting problem. Although these conditions are related to the surface energy of the liquid, there is not a straightforward manner for calculating the surface tension from the drop features. Nonetheless, the drop dimensions may be obtained through interferometric measurements and thus a mathematical relationship might be established in the future.

The basis for our measurements is the analysis of the interferometric signal generated at the tip of an optical fiber with a drop of liquid. A schematic of the optical arrangement used in our experiments is shown in Fig. 1(b). After dipping the cleaved end of an optical fiber into a liquid, a remnant-pendant drop is formed. The drop size and the refractive index of the liquid will generate an interferometric signal that may be monitored via the back-reflected light. Although the signal will mainly provide information regarding the refractive index and the drop size, the process of drop formation is closely related to physical characteristics of the liquid, namely, surface tension and viscosity (see Fig. 2). Thus, the final volume of the drop will contain information about these features.

#201124 - $15.00 USD Received 11 Nov 2013; revised 16 Jan 2014; accepted 27 Jan 2014; published 3 Feb 2014

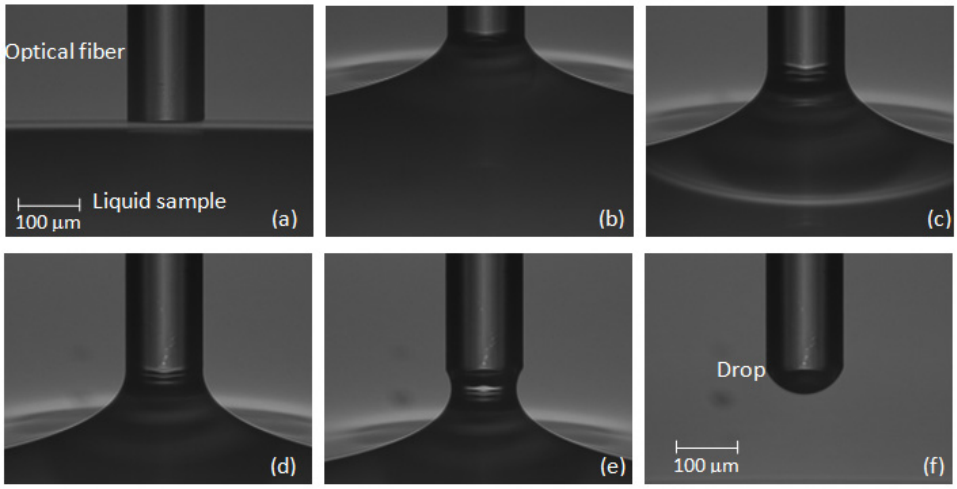

Fig. 2. A set of pictures of the wetting process: the optical fiber is initially in close proximity to the liquid (a) and subsequently immersed into it and extracted at regular intervals (b-e). Once the fiber is out of the liquid sample, a remnant-pendant drop is formed at the fiber end face (f). The wetting process with a DMS liquid (Media 1) is different than that of glycerin (Media 2).

For a static stress analysis, the contact angle (CA) of a sessile drop is typically related to the surface properties of the liquid and the solid [1, 6, 17]. However, the CA for a remnant drop formed at the tip of an optical fiber is always larger than that of a typical sessile drop (see Fig. 1). This is important since there is not a straightforward manner for estimating the size of the drop. For our experimental condition, the radii of curvature of the drops are smaller than their corresponding capillary lengths, thus droplets take the shape of spherical caps and the effects of gravity can be neglected; under these conditions, the main role in drop formation may be attributed to capillary forces [1]. Since the capillary forces define the drop shape, the surface tension of the liquid may be determined upon measuring the height of the drop.

3. Experimental setup

The experimental procedure for drop formation consists on dipping the cleaved end of an optical fiber into a liquid sample to form a remnant-pendant drop. One end of a standard single-mode optical fiber (Corning SMF-28e +) is connected to a spectral interrogator (FBG interrogator, Micron Optics sm125); the polymer coating at the other end is removed, then the fiber is cleaved and positioned vertically facing downwards to the liquid sample. The latter is placed on a microscope slide –to form a sessile drop-, whose position and displacement are controlled by means of a mechanical actuator (Zaber T-LA60A). To wet the fiber, the sample is raised until the fiber end is completely immersed; subsequently, the sample goes down to take the fiber out from the sample and a drop is formed at the fiber tip (see Fig. 2).

Several things are to be considered during the drop formation process. In contrast to previous reports [18], the liquid sample volume is much larger than that of the final drop formed at the tip of the fiber. For all the experiments, the initial volume on the microscope slide for the tested liquids (see bottom part of the pictures in Fig. 2) was around 4 µL. Upon comparing this volume with the typical drop volumes obtained with our setup (200-300 pL), we obtain a volume ratio (V_{sample}/V_{drop}) in the order of 10^4. We verified experimentally that this volume ratio, and under the withdrawal speeds used in our setup (see below), consistent results are obtained for the drop sizes formed at the tip of the fiber.

#201124 - $15.00 USD Received 11 Nov 2013; revised 16 Jan 2014; accepted 27 Jan 2014; published 3 Feb 2014

The speed at which the optical fiber is withdrawn from the liquid is also an important parameter: features such as viscosity, density and surface tension of the liquid play an important role in determining this characteristic speed [1], which may be estimated as:

$$V^* = \frac{\gamma}{\eta}. \tag{1}$$

This expression relates the surface tension (γ) with the dynamic viscosity of the liquid (η); relevant data for estimating the characteristic speed for the liquids used in our experiments is given in Table 1. Simple calculations yield a maximum withdrawal speed of about 2.2 mm/s, which corresponds to the most viscous liquid used in our experiments. The withdrawal speed of the fiber was controlled via software and the mechanical actuator displacing the liquid sample in steps of 1 μm; at each step, the sample was left to rest for 10 s. Under these conditions, the drop formation at the tip of the optical fiber should not depend on the viscosity of the liquid. Thus, the drop features can be mostly attributed to the surface tension of the liquid sample.

The remnant-pendant drop at the tip of the fiber generates an interferometric signal due to the refractive index difference between the fiber and the liquid. Monitoring of the interference pattern for each liquid can be readily performed with the FBG interrogator and, with proper signal analysis, the drop features (e.g., height) can be obtained. During the wetting process and while acquiring the interferometric signals, a CCD camera is also used to record side view images of the fiber-drop arrangement. Additionally, temperature and humidity are also recorded for each experiment by means of a resistance temperature detector (RTD) and a hygrometer, respectively. The experimental arrangement is fully enclosed within an acrylic box to prevent perturbations from environmental fluctuations. Finally, control and data acquisition are conveniently done via a virtual instrument programmed in LabView.

4. Theoretical analysis

The fiber-liquid and liquid-air interfaces formed at the optical fiber tip can be considered as the reflecting surfaces in a two-mirror Fabry-Perot interferometer (2MFPI). However, the optical arrangement is often prone to have a third reflecting surface, far from the drop, to form a three-mirror arrangement (3MFPI). The drop features are thus obtained by means of a multi-mirror Fabry-Perot (MMFPI) model using the refractive indices of the corresponding media [20, 21].

Our analysis of the MMFPI follows the usual matrix formalism of multilayer films, neglecting losses due to absorption, scattering, misalignment, and diffraction [20, 21]. Consider N partially transmitting, plane parallel mirrors of zero thickness, and sequentially numbered $i = 1, 2, \ldots N$. The mirrors can be analyzed as pairs of consecutive mirrors and subsequently may be used to form stacks, as shown in Fig. 3. Following the notation given in the figure, E_i^+ is the amplitude of the electric-field vector on the left hand side of mirror i for a wave front propagating to the right; E_i^- is the amplitude of the left hand side of mirror i for a wave front traveling to the left. r_i and t_i are the amplitude reflection and transmission coefficients for mirror i; the distance from mirror i to mirror $(i + 1)$ is L_i, contained in the expression for the optical phase length $\varphi_i = 2\pi L_i / \lambda$.

#201124 - $15.00 USD Received 11 Nov 2013; revised 16 Jan 2014; accepted 27 Jan 2014; published 3 Feb 2014

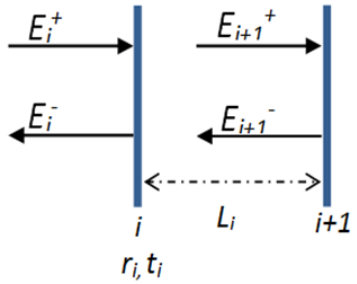

Fig. 3. Amplitudes at mirrors *i* and *i + 1* out of a stack of *N* mirrors.

For two mirrors i and (i + 1) we find that

$$E_{i+1}^{+}e^{-i\varphi_i} = t_i E_i^{+} + E_{i+1}^{-} r_i e^{i\varphi_i} \tag{2}$$

and

$$E_i^{-} = -E_i^{+} r_i + E_{i+1}^{-} t_i e^{i\varphi_i}. \tag{3}$$

From Eq. (2) we obtain

$$E_i^{+} = \frac{1}{t_i} E_{i+1}^{+} e^{-i\varphi_i} - \frac{r_i}{t_i} E_{i+1}^{-} e^{i\varphi_i}, \tag{4}$$

and substituting in (3)

$$E_i^{-} = -\frac{r_i}{t_i} E_{i+1}^{+} e^{-i\varphi_i} + \frac{1}{t_i} E_{i+1}^{-} e^{i\varphi_i}. \tag{5}$$

Equations (4) and (5) can be expressed in matrix form as

$$\begin{pmatrix} E_i^{+} \\ E_i^{-} \end{pmatrix} = \frac{1}{t_i} \begin{bmatrix} e^{-i\varphi_i} & -r_i e^{i\varphi_i} \\ -r_i e^{-i\varphi_i} & e^{i\varphi_i} \end{bmatrix} \begin{pmatrix} E_{i+1}^{+} \\ E_{i+1}^{-} \end{pmatrix}. \tag{6}$$

For a series of *N* mirrors, the corresponding matrix equation reads:

$$\begin{pmatrix} E_1^{+} \\ E_1^{-} \end{pmatrix} = \frac{1}{t_1 t_2 \ldots t_{N-1}} \begin{bmatrix} e^{-i\varphi_1} & -r_i e^{i\varphi_1} \\ -r_i e^{-i\varphi_1} & e^{i\varphi_1} \end{bmatrix} \times \begin{bmatrix} e^{-i\varphi_2} & -r_i e^{i\varphi_2} \\ -r_i e^{-i\varphi_2} & e^{i\varphi_2} \end{bmatrix} \times \ldots \times \begin{bmatrix} e^{-i\varphi_{N-1}} & -r_i e^{i\varphi_{N-1}} \\ -r_i e^{-i\varphi_{N-1}} & e^{i\varphi_{N-1}} \end{bmatrix} \begin{pmatrix} E_N^{+} \\ E_N^{-} \end{pmatrix} \tag{7}$$

or equivalently:

$$\begin{pmatrix} E_i^{+} \\ E_i^{-} \end{pmatrix} = \frac{1}{t_1 t_2 \ldots t_{N-1}} \begin{bmatrix} A & B \\ C & D \end{bmatrix} \begin{pmatrix} E_N^{+} \\ E_N^{-} \end{pmatrix}, \tag{8}$$

where *A*, *B*, *C*, and *D* are the coefficients of the resulting matrix; E_N^{+} and E_N^{-} are the amplitudes of the electric field vector on the left side of mirror *N* propagating to the right and the left, respectively. Using these expressions, the reflectance of *N* parallel, partially transmitting plane mirrors without absorption can be calculated as the ratio $r = E_i^{-} / E_i^{+}$. Using (8) and considering consecutive mirrors *i* and *i + 1* we obtain:

#201124 - $15.00 USD Received 11 Nov 2013; revised 16 Jan 2014; accepted 27 Jan 2014; published 3 Feb 2014

$$r = -\frac{r_{i+1} + r_i e^{-2i\varphi_i}}{r_i r_{i+1} + e^{-2i\varphi_i}}. \tag{9}$$

The reflection intensity coefficient is then given by the product $R = r\,r^*$, where r^* is the complex conjugate of r. Thus, for a two mirror Fabry-Perot interferometer (2MFPI), the intensity reflection is given by

$$R_{2M} = \frac{r_1^2 + r_2^2 + 2r_1 r_2 \cos[2\varphi_1]}{1 + r_1 r_2 (r_1 r_2 + 2\cos[2\varphi_1])}. \tag{10}$$

And, for a three mirror Fabry-Perot interferometer (3MFPI), the intensity reflection is

$$R_{3M} = \frac{r_2^2 + r_3^2 + r_1^2 (1 + r_2^2 r_3^2) + Q}{1 + r_2^2 r_3^2 + r_1^2 (r_2^2 + r_3^2) + Q}, \tag{11}$$

where

$$\begin{aligned} Q = {} & 2r_2 \left(r_1 (1 + r_3^2) \cos[2\varphi_1] + r_1 r_2 r_3 \cos[2\varphi_1 - 2\varphi_2] + (1 + r_1^2) r_3 \cos[2\varphi_2] \right) \\ & + 2r_1 r_3 \cos[2(\varphi_1 + \varphi_2)] \end{aligned} \tag{12}$$

At the drop-air interface, the mirror is a curved reflecting surface, and several assumptions are made in the model. The divergence of the beam crossing the fiber-liquid interface is small due to the refractive indices of the liquids used in our experiments, which are close to the fiber core refractive index (1.4682). Considering a small index difference, the numerical aperture for this interface is also small and the spot diameter at the edge of the drop would be about two times the size of the fiber core. Thus, as a first approximation, if the drops have at least a radius of curvature close to radius of the optical fiber, the distant edge of the drop can be considered as a plane surface. In our experiments, the height of the drop (h) is obtained upon fitting the FBG interrogator data either to the two-mirror (2M) or three-mirror (3M) reflectivities (Eqs. (10) and (11), respectively). The nonlinear fitting thus yields the values for the reflectivities at each interface together with the height of the drop.

5. Results and discussion

The liquids used in our experiments were three different dimethylsiloxanes (Gelest, DMS-T23, DMS-T31 and DMS-T41) [22] and glycerin [23, 24]. The selected liquids are stable, non-volatile liquids and with well-known physical properties, some of which are listed in Table 1.

Table 1. Physical Properties of the Liquids

Liquid	Surface tension [mN/m]	Specific gravity	Refractive index	Viscosity [cSt]
DMS-T23	21.1	0.970	1.4031	350
DMS-T31	21.2	0.971	1.4034	1000
DMS-T41	21.5	0.974	1.4035	10000
Glycerin	62.5	1.25	1.474	934

The wetting process and drop formation were evaluated following two different procedures: cleaving the fiber for every wetting event and using the same fiber for each subsequent test after proper cleaning. For each liquid the wetting process was repeated twice and data were collected for two interferometric configurations: a two-mirror (2M) and a three-mirror (3M) arrangement. For the 2M configuration, after the remnant drop is formed, a non-reflecting wedged black anodized aluminum piece was placed below the drop to avoid

#201124 - $15.00 USD Received 11 Nov 2013; revised 16 Jan 2014; accepted 27 Jan 2014; published 3 Feb 2014

any additional back reflection. For the 3M arrangement, the third reflecting surface was an infrared mirror (Thorlabs, BB05-E04, R>99%) placed underneath the drop.

Figure 4 illustrates the two drops configurations analyzed as interferometric arrangements with two (a) and three (b) reflective surfaces. Figure 4(c) shows an example of the experimental signals acquired for the DMS-T41 liquid. While the signal showing a larger period (blue) corresponds to the 2M configuration, the signal with the shorter period (red) corresponds to the 3M interferometric arrangement.

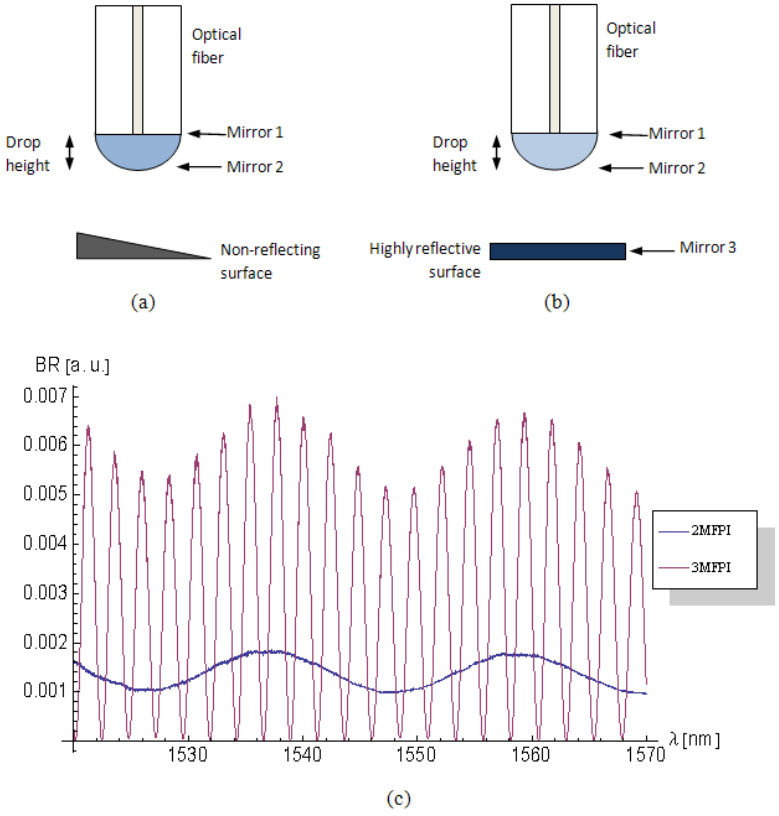

Fig. 4. Schematic representation of: (a) 2MFPI arrangement, (b) 3MFPI arrangement and (c) typical back-reflected (BR) interference signals obtained for each case.

The drop height is obtained from the phase of the Fabry-Perot theoretical model ($\varphi_i = 2\pi L_i / \lambda$), after fitting the experimental data to Eq. (10) or Eq. (11). For both cases, the drop height corresponds to L_1, which can be readily obtained after fitting the remaining parameters used in the model.

Table 2 summarizes some results; one of the main characteristics of the three dimethylsiloxanes (DMSs) is their similarity in surface tension, refractive index, and specific weight (see Table 1). Notice that for these three liquids, the values of drop height obtained after data analysis is very similar. This is consistent with the assumption that the drop height for the wetting procedure is mostly determined by the surface tension of the liquid, which in some way is balanced with the drop weight. In contrast, for glycerin the average values of drop heights are noticeably larger than those of the DMSs. Note that glycerin has a larger value of surface tension compared to the DMSs.

#201124 - $15.00 USD Received 11 Nov 2013; revised 16 Jan 2014; accepted 27 Jan 2014; published 3 Feb 2014

Table 2. Drop Height for Two Mirrors (2M) and Three Mirrors (3M) Interferometric Configurations*

Liquid	Drop 1 Cleaved [μm]		Drop 2 Cleaved [μm]		Drop 1 Cleaned [μm]	Drop 2 Cleaned [μm]
	2M	3M	2M	3M	2M	2M
DMS-T23	38.29	38.35	39.07	39.08	36.35	36.93
DMS-T31	38.85	39.48	38.57	38.73	37.17	37.10
DMS-T41	38.88	38.89	38.93	38.38	38.20	38.93
Glycerin	42.95	41.86	42.19	41.92	43.19	41.19

*The first two columns show results for two different wetting processes using different cleaved sections for each measurement. Drop heights for two wetting processes after cleaning the same fiber are shown in the last two columns.

While the DMSs liquids have very similar values of the surface tension and their viscosities differ significantly, glycerin has a higher surface tension value. The backreflected signals were acquired and the data were fitted to the 2M and 3M models. A plot with the resulting drop heights for all the liquids is shown in Fig. 5; both models provide very similar results for the same wetting events. Remarkably, the results suggest that the contribution to the height of the drop due to viscosity is almost negligible, since the DMSs samples possess very different viscosities.

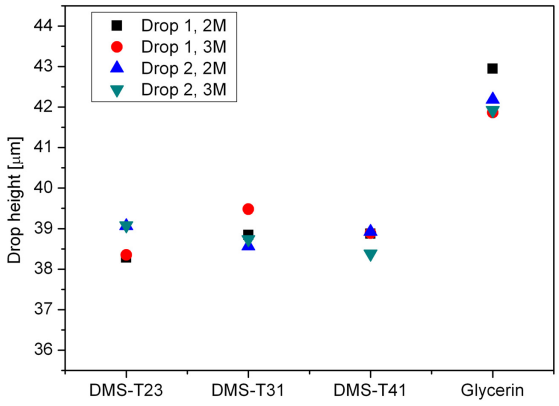

Fig. 5. Drop heights for different liquids obtained with 2M and 3M models; the fibers were cleaved before each dipping event.

The wetting process of the fiber can be affected by the presence of surfactants —which is very difficult to control in common liquids— and possible surface and edge imperfections at the fiber end-face due to cleaving. These effects were evaluated performing drop height measurements using the same optical fiber following a cleaning procedure before each test. The fiber was carefully cleaned by immersing it subsequently in acetone, methylene chloride and finally, in deionized water. A final inspection of the fiber tip was also made using the CCD camera. Since data fitting yields similar results for the 2M and 3M configurations, only the 2M model was used for drop height calculations. Figure 6 shows the values of drop heights obtained for this set of experiments.

#201124 - $15.00 USD Received 11 Nov 2013; revised 16 Jan 2014; accepted 27 Jan 2014; published 3 Feb 2014

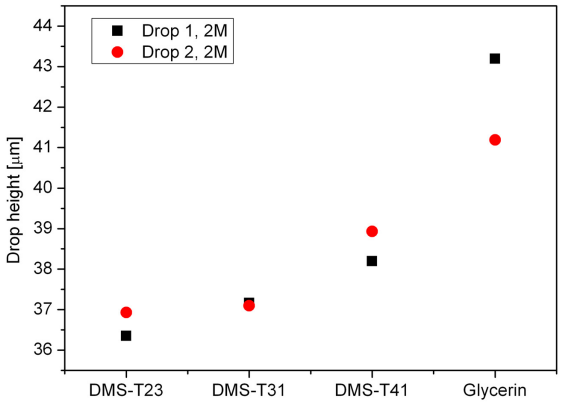

Fig. 6. Drop height for different liquids using the same fiber.

Upon comparing the drop heights obtained with both methods (i.e., cleaving and cleaning the fiber tip), the calculated drop heights seem to yield slightly different results. Solid substrates always present some degree of adsorption of gas or vapor at the solid-gas interface; for vapors close to the saturation pressure, the amount of adsorption can be quite large and may reach or exceed the point of monolayer formation thereby changing the solid-gas interfacial energy [17]. In general, the materials used in surface tension measurements are not affected by the acids, bases and organic solvents used in the cleaning process [19]. However, the drop heights measured when using the cleaned optical fiber yielded smaller drops. This systematic deviation is caused by the different surface wetting properties after the cleaning process. Even though both procedures result in different drop heights for the same liquid, the results from both cases show to be consistent for detecting liquids with different surface tensions. The surface tension sensitivity of the proposed technique may provide relevant information to derive a theoretical model for the drop shape, including considerations of the wetting properties of the optical fiber.

In our experiments, glycerin was used due to its high surface tension compared to the DMSs liquids. As seen in Figs. 5 and 6, this surface tension difference yields different drop heights thereby validating the proposed measurement technique. However, although it has an apparent stable behavior for this purpose, glycerin is highly hygroscopic and its physical properties are prone to changes due to water absorption. This condition changes the surface tension since the liquid becomes a solution –glycerin and water–, whose surface tension would fall somewhere between that of water (72.7 mN/m) and glycerin. This is evident in Fig. 6, showing different drop height measurements for glycerin obtained for the wetting of the same cleaned fiber.

In general, surface tension measurements can lead to different results depending on the measuring methods, and mainly due to mathematical analysis of complex phenomena; however, surface tension of a pure liquid must always be the same [17]. In practice, the goal is oftentimes to determine changes in surface tension rather than obtaining absolute values. With the proposed technique detection of variations or differences in the surface tension of liquids is feasible and thus can be useful for this purpose. As a first approximation, these preliminary results confirm that surface tension is the main contributor to the size of a remnant drop formed by dipping an optical fiber into a liquid sample. This will hold for controlled wetting conditions such as those followed in our experiments. To the best of our knowledge, there is no evidence of a detailed study of this particular wetting arrangement (i.e., a remnant-pendant drop constrained by a finite surface). As such, a direct relation between drop height and surface tension for our configuration is not yet available. The geometry constrains and the scales of the drop and fiber cross-section seem to impose

#201124 - $15.00 USD Received 11 Nov 2013; revised 16 Jan 2014; accepted 27 Jan 2014; published 3 Feb 2014

wetting conditions for which conventional analysis cannot be applied (e.g., the Young-Laplace model). In addition, other contributions to drop formation might also be relevant, such as the effects of the contact line and the adhesion at the fiber-liquid interface [1, 6, 17, 25, 26]. In spite of these limitations for data analysis, we believe that the proposed technique offers attractive features for liquid analysis such as small volume sample, which is key for small-scale chemical analysis systems.

6. Conclusions

We have demonstrated a technique to evaluate surface tension differences in liquid samples. Our results show that the height of a drop formed at the tip of an optical fiber under controlled wetting conditions is directly correlated to the surface tension of the liquid. The proposed configuration may provide relevant information of physical properties of liquids using volumes within the picoliters range. In general the setup is simpler than other techniques based on pendant drop analysis and is based on the analysis of a steady drop. Further studies of the wetting process may lead to the simultaneous determination of other physical properties of the liquids (e.g., viscosity, refractive index, volatility), as well as the characterization of solutions or indirect detection of contaminants in liquids from the measurement of physical properties. This might be of interest for developing label-free chemical or biological sensors, as well as opto- and microfluidics systems.

Acknowledgments.

This was supported in part by DGAPA-UNAM through grant PAPIIT-IN102112, PAEP-UNAM and CONACyT through grant 154464. The authors are thankful to R. Zenit, A. Minzoni, and E. Geffroy for their invaluable advice and useful discussions.